Reionization: characteristic scales, topology and observability

**Ilian T. Iliev · Ue-Li Pen · Patrick McDonald ·
Paul R. Shapiro · Garrelt Mellema · Marcelo A. Alvarez**

Abstract Recently the numerical simulations of the process of reionization of the universe at $z > 6$ have made a qualitative leap forward, reaching sufficient sizes and dynamic range to determine the characteristic scales of this process. This allowed making the first realistic predictions for a variety of observational signatures. We discuss recent results from large-scale radiative transfer and structure formation simulations on the observability of high-redshift Ly-α sources. We also briefly discuss the dependence of the characteristic scales and topology of the ionized and neutral patches on the reionization parameters.

I.T. Iliev (✉) · U.-L. Pen · P. McDonald
Canadian Institute for Theoretical Astrophysics, University of Toronto, 60 St. George Street, Toronto, ON M5S 3H8, Canada
e-mail: iliev@physik.uzh.ch

I.T. Iliev
Institut für Theoretische Physik, Universität Zürich, Winterthurerstrasse 190, 8057 Zürich, Switzerland

P.R. Shapiro
Department of Astronomy, University of Texas, Austin, TX 78712-1083, USA

G. Mellema
Stockholm Observatory, AlbaNova University Center, Stockholm University, 106 91 Stockholm, Sweden

M.A. Alvarez
Kavli Institute for Particle Astrophysics and Cosmology, Stanford University, Stanford, CA 94305, USA

1 Introduction

The observations of high-redshift QSO's (Fan and et al. 2001; Becker and et al. 2001) and large-scale CMB polarization (Spergel et al. 2007) indicate that the intergalactic medium has been completely ionized by redshift $z \sim 6$ through an extended process. The most probable cause was the ionizing radiation of the First Stars and QSO's. Currently these are the two main direct observational constraints on this epoch. This scarcity of observational data is set to change dramatically in the next few years, however. A number of large observational projects are currently under way, e.g. observations at the redshifted 21-cm line of hydrogen e.g. (Madau et al. 1997; Tozzi et al. 2000; Iliev et al. 2002; Mellema et al. 2006; Furlanetto et al. 2006), detection of small-scale CMB anisotropies due to the kinetic Sunyaev-Zel'dovich (kSZ) effect e.g. (Hu 2000; Santos et al. 2003; Iliev et al. 2007b), and surveys of high-redshift Ly-α emitters and studies of the IGM absorption e.g. (Rhoads et al. 2003; Stanway et al. 2004; Bunker et al. 2006). The planning and success of these experiments relies critically upon understanding the large-scale geometry of reionization, i.e. the size- and spatial distribution of the ionized and neutral patches. This is best derived by large-scale simulations, although a number of semi-analytical models exist as well e.g. (Furlanetto et al. 2004). Recently we presented the first large-scale, high-resolution radiative transfer simulations of cosmic reionization (Iliev et al. 2006, 2007a) and applied those to derive a range of reionization observables (Mellema et al. 2006; Iliev et al. 2007b, 2007c, 2008; Holder et al. 2007; Doré et al. 2007). Subsequently, (Zahn et al. 2007; Trac and Cen 2007) performed large-scale reionization simulations (in $64/h$–$100/h$ Mpc simulation boxes) using methodology similar to ours, but utilizing different radiative trans-

Fig. 1 Large-scale geometry of reionization and the local variations in reionization history as seen at redshifted 21-cm line: (*top*) lg(δT_b) and (*bottom*) δT_b smoothed with $3'$ compensated Gaussian beam, both in units of mK
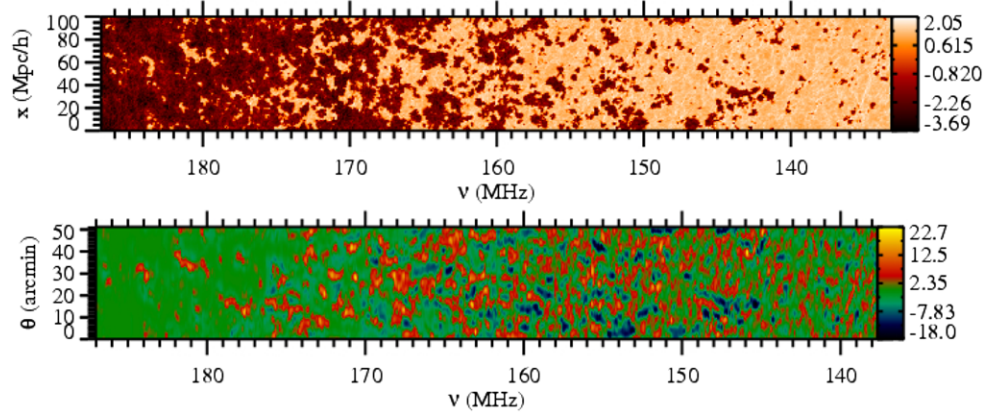
fer and *N*-body methods and applied them to studies of the reionization characteristics and observable signatures. Here we summarize our recent results on the characteristic scales and topology of reionization and implications of our simulations for the observability of high-redshift Ly-α sources.

2 Characteristic scales of reionization

The characteristic scales of the ionization and density fluctuations are directly imprinted in the fluctuations of all reionization observables (Fig. 1). It is thus critical to understand what these scales are and their dependencies on the (largely unknown) reionization parameters. We investigated the dependence of the characteristic sizes of ionized and neutral patches on some basic properties of the sources of reionization and the intergalactic medium, such as the halo mass-to-light ratio, susceptibility of haloes to positive and negative feedback, and the gas clumping at small scales. We used two independent methods for identifying the size distribution of patches, the friends-of-friends (FOF) method (Iliev et al. 2006), where all topologically-connected ionized regions are considered as one region, and the spherical average method (Zahn et al. 2007), where an averaging over a spherical region and an ionization threshold are used to define the size. In the FOF method, throughout most of the evolution there is one very large connected region in which most of the volume is contained. For the spherical average method, the bubble distribution typically peaks on Mpc scales. Suppression of ionizing sources within ionized regions and gas clumping both reduce the size and increase the number of H II regions, although the effect is modest, reducing the typical radius of H II regions by factors of at most a few (Fig. 2). We also found that density and ionized fraction are correlated on large scales, regardless of the degree of clumping and suppression. The genus of the ionization field proved to be much more sensitive to suppression and clumping than the size distributions or the power spectra and could thus be

used for more detailed characterization of the reionization parameters. We will present these results in detail in an upcoming paper (Alvarez et al., in prep.).

3 High-redshift Ly-α sources

Observations of the high-redshift Ly-α sources have provided us with a wealth of information about the state of the IGM and the nature of the galaxies at the end of reionization and hold even more promise for the future. In addition to probing the IGM and the source luminosity function (and thus, indirectly, the halo mass function and ionization source properties), they may also be used to constrain the reionization topology (Rhoads 2007). The first rare objects form in the highest peaks of the density field. The statistics of Gaussian fields predicts that such peaks are strongly clustered at high redshift. Hence each high-redshift, massive galaxy was surrounded by numerous smaller ionizing sources. The self-consistent simulations of such regions require following a large volume while also resolving the low-mass halos driving reionization.

In Fig. 3 we illustrate several stages of the reionization history of a high density peak. The most massive source in our volume (at $z = 6$) is shifted to the center using the periodicity of the computational box. At redshift $z = 12.9$ the source is invisible due to the damping wing from the neutral gas outside the small H II region. By redshift $z = 9$ many more haloes have formed, most of them in large clustered groups. The H II region surrounding the central peak is among the largest, but the central source emission remains strongly affected by damping. Only by redshift $z = 8$ the ionized region is large enough to render the source potentially visible. The reionization geometry becomes quite complex, most ionized bubbles are interconnected, but large neutral patches remain between them, which is also showing in the topological characteristics of the filed like the genus discussed above. Finally, by the nominal overlap $z = 6.6$

Fig. 2 Ionization maps (*blue* neutral, *red* ionized) of selected $100 \, h^{-1}$ Mpc box simulations at half-ionized epoch for high (*bottom panels*) and low source efficiencies (*top*) and with (*right panels*) and without (*left panels*) sub-grid clumping. All simulations use the same N-body and radiative transfer resolution
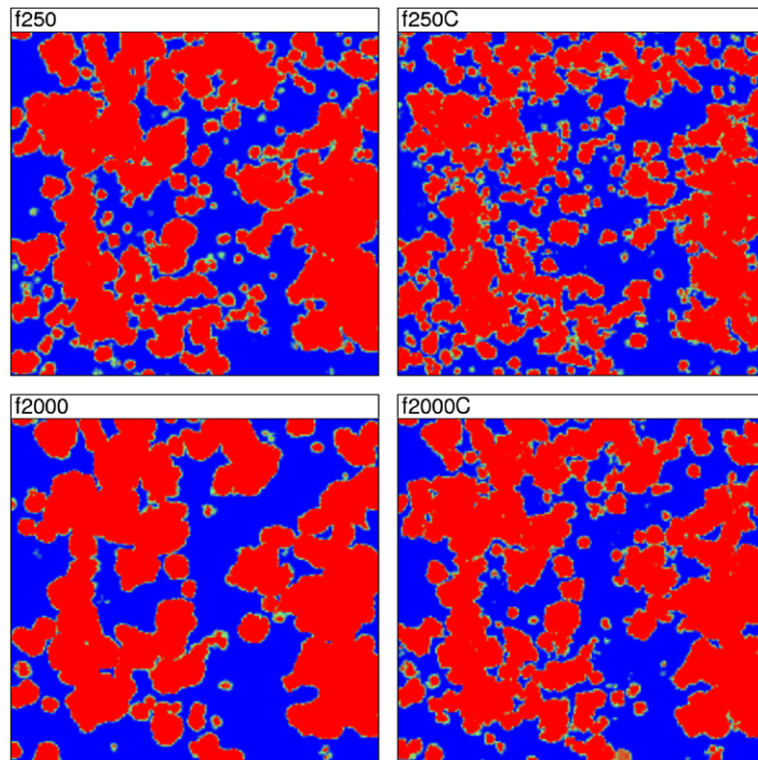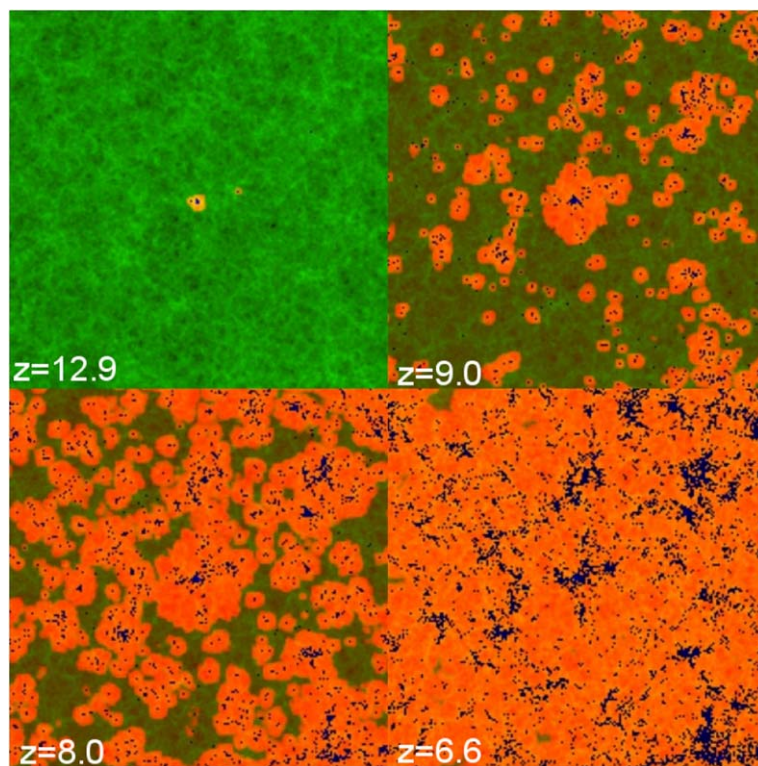
Fig. 3 The reionization history of a high density peak. The images are centered on the most massive (at $z = 6$) halo in our computational volume and are of size $100 \, h^{-1}$ Mpc to the side. The cosmological density field (*dark, green*) is superimposed with the ionized fraction (*light, orange*) and the ionizing sources (*dark dots*)

all ionized regions have merged into one topologically-connected region, although substantial neutral patches remain interspersed throughout our volume, which is still largely optically-thick to both Ly-α and ionizing radiation.

Only by $z \sim 6$ this volume becomes on average optically-thin to ionizing radiation. The last statement is resolution-dependent, however. While the mean IGM does become optically-thin, after overlap the mean free path of ionizing
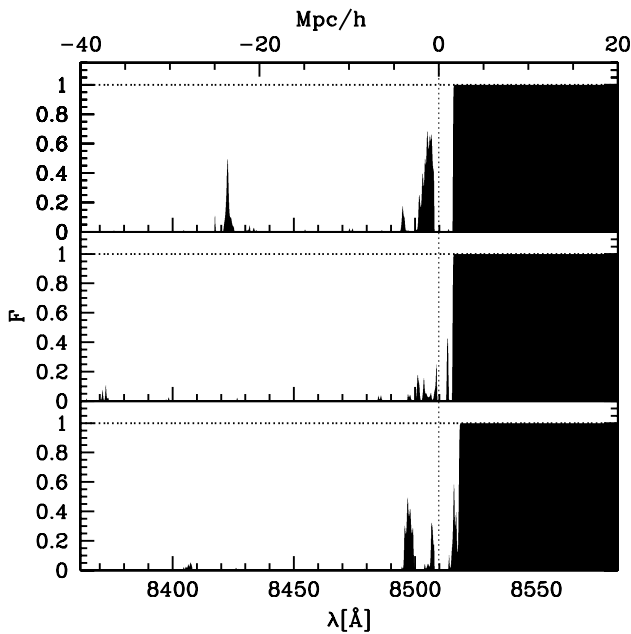
Fig. 4 Ly-α sources at redshift $z = 6.0$: Transmission factor along sample lines-of-sight vs. λ/comoving distance from the most massive galaxy ($M/\sim 10^{12} M_\odot$ at $z = 6$) in our volume. There is significant transmission in the proximity zone and transmission gaps in the mean IGM away from the source. Gas infall results in some absorption red-ward of the line center

Fig. 5 Ly-α sources at redshift $z = 6.0$: Luminosity function without (*black*) and with absorption included (*red*). For reference, the *green, dotted line* shows the result suppressing each source by 50%, which would be the case if e.g. all of the blue wing of the emission line, but none of the red wing is absorbed

photons is determined by small-scale, self-shielded systems (Damped Lyman-α and Lyman Limit systems) which are not resolved in the current simulation. Thus the mean free path could be shorter, of order few tens of comoving Mpc, only rising to 100 Mpc by $z \sim 3$.

In Fig. 4 we show some sample absorption spectra for the same luminous source. The spectra exhibit extended high-transmission (10–60% transmission) regions in the highly-ionized proximity zone of the luminous source, within $5\,h^{-1}$ Mpc (~ 20 Å). The center of the peak itself is optically-thick due to its high density. The infall around the central peak blue-shifts photons, resulting in some transmission behind the redshift-space position of the source. Away from the proximity region the absorption is largely saturated, but there are a number of transmission gaps with up to a few per cent transmission. In Fig. 5 we show the Ly-α source luminosity function at the same redshift. For the weaker sources roughly half of the intrinsic luminosity is transmitted (the red wing of the line), while the most luminous sources suffer from additional absorption due to the gas infall that surrounds them. Further complications arise because such a massive galaxy could host a QSO in addition to the stellar sources present. Furthermore, such luminous Ly-α sources are expected to be strongly dust-obscured e.g. (Tilvi et al. 2008). Future work will quantify the statistics of these features and its evolution.
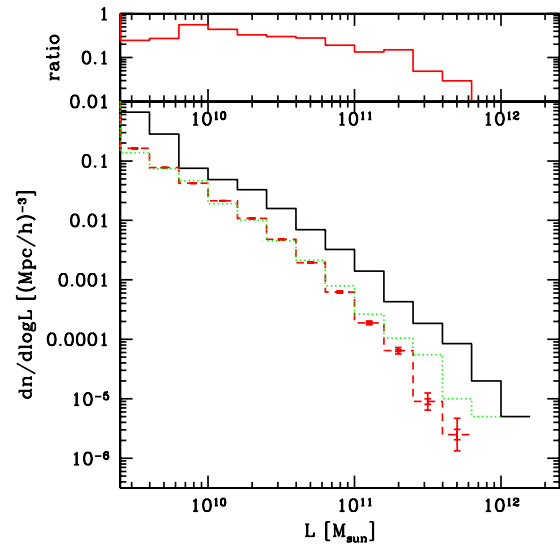
References

Becker, R.H., et al.: Evidence for reionization at $z \sim 6$: detection of a Gunn-Peterson trough in a $z = 6.28$ Quasar. Astron. J. **122**, 2850–2857 (2001). doi:10.1086/324231

Bunker, A., Stanway, E., Ellis, R., McMahon, R., Eyles, L., Lacy, M.: Star forming galaxies at $z \sim 6$ and reionization. New Astron. Rev. **50**, 94–100 (2006). doi:10.1016/j.newar.2005.11.006

Doré, O., Holder, G., Alvarez, M.A., Iliev, I.T., Mellema, G., Pen, U.L., Shapiro, P.R.: Signature of patchy reionization in the polarization anisotropy of the CMB. Phys. Rev. D **76**(4), 043002 (2007). doi:10.1103/PhysRevD.76.043002

Fan, X., et al.: A survey of $z > 5.8$ quasars in the Sloan digital sky survey. I. Discovery of three new quasars and the spatial density of luminous quasars at $z \sim 6$. Astron. J. **122**, 2833–2849 (2001). doi:10.1086/324111

Furlanetto, S.R., Zaldarriaga, M., Hernquist, L.: The growth of H II regions during reionization. Astrophys. J. **613**, 1–15 (2004)

Furlanetto, S.R., Oh, S.P., Briggs, F.H.: Cosmology at low frequencies: The 21 cm transition and the high-redshift universe. Phys. Rep. **433**, 181–301 (2006). doi:10.1016/j.physrep.2006.08.002

Holder, G.P., Iliev, I.T., Mellema, G.: Reconstructing the Thomson optical depth due to patchy reionization with 21 cm fluctuation maps. Astrophys. J. Lett. **663**, L1–L4 (2007). doi:10.1086/519835

Hu, W.: Reionization revisited: secondary cosmic microwave background anisotropies and polarization. Astrophys. J. **529**, 12–25 (2000). doi:10.1086/308279

Iliev, I.T., Shapiro, P.R., Ferrara, A., Martel, H.: On the direct detectability of the cosmic dark ages: 21 centimeter emission from minihalos. Astrophys. J. Lett. **572**, L123–L126 (2002)

Iliev, I.T., Mellema, G., Pen, U.L., Merz, H., Shapiro, P.R., Alvarez, M.A.: Simulating cosmic reionization at large scales—I. The geometry of reionization. Mon. Not. R. Astron. Soc. **369**, 1625–1638 (2006). doi:10.1111/j.1365-2966.2006.10502.x

Iliev, I.T., Mellema, G., Shapiro, P.R., Pen, U.L.: Self-regulated reionization. Mon. Not. R. Astron. Soc. **376**, 534–548 (2007a). doi:10.1111/j.1365-2966.2007.11482.x

Iliev, I.T., Pen, U.L., Bond, J.R., Mellema, G., Shapiro, P.R.: The kinetic Sunyaev-Zel'dovich effect from radiative transfer simulations of patchy reionization. Astrophys. J. **660**, 933–944 (2007b). doi:10.1086/513687

Iliev I.T., Shapiro P.R., Mellema G., Pen U.L., McDonald P., Bond J.R.: Simulating reionization: character and observability. ArXiv e-prints, 708 (2007c)

Iliev I.T., Mellema G., Pen U.L., Bond J.R., Shapiro P.R.: Current models of the observable consequences of cosmic reionization and their detectability. Mon. Not. R. Astron. Soc. **77** (2008). doi:10.1111/j.1365-2966.2007.12629.x

Madau, P., Meiksin, A., Rees, M.J.: 21 centimeter tomography of the intergalactic medium at high redshift. Astrophys. J. **475**, 429 (1997)

Mellema, G., Iliev, I.T., Pen, U.L., Shapiro, P.R.: Simulating cosmic reionization at large scales—II. The 21-cm emission features and statistical signals Mon. Not. R. Astron. Soc. **372**, 679–692 (2006). doi:10.1111/j.1365-2966.2006.10919.x

Rhoads J.E.: Testing the topology of reionization. ArXiv e-prints, 708 (2007)

Rhoads, J.E., et al.: Spectroscopic confirmation of three redshift $z \sim 5.7$ Ly-α emitters from the large-area Lyman alpha survey. Astron. J. **125**, 1006–1013 (2003). doi:10.1086/346272

Santos, M.G., Cooray, A., Haiman, Z., Knox, L., Ma, C.P.: Small-scale cosmic microwave background temperature and polarization anisotropies due to patchy reionization. Astrophys. J. **598**, 756–766 (2003). doi:10.1086/378772

Spergel, D.N., et al.: Three-year Wilkinson microwave anisotropy probe (WMAP) observations: Implications for cosmology. Astrophys. J. Suppl. Ser. **170**, 377–408 (2007). doi:10.1086/513700

Stanway, E.R., et al.: Three Ly-α emitters at $z \sim 6$: early GMOS/Gemini data from the GLARE project. Astrophys. J. Lett. **604**, L13–L16 (2004). doi:10.1086/383523

Tilvi, V., Malhotra, S., Rhoads, J., Scannapieco, E., Iliev, I.T., Mellema, G.: A simple physical model for Lyman alpha emitters. Astrophys. J. Lett. (2008, submitted)

Tozzi, P., Madau, P., Meiksin, A., Rees, M.J.: Radio signatures of H I at high redshift: mapping the end of the "Dark Ages". Astrophys. J. **528**, 597–606 (2000)

Trac, H., Cen, R.: Radiative transfer simulations of cosmic reionization. I. Methodology and initial results. Astrophys. J. **671**, 1–13 (2007). doi:10.1086/522566

Zahn, O., Lidz, A., McQuinn, M., Dutta, S., Hernquist, L., Zaldarriaga, M., Furlanetto, S.R.: Simulations and analytic calculations of bubble growth during hydrogen reionization. Astrophys. J. **654**, 12–26 (2007). doi:10.1086/509597